Journal Pre-proofs

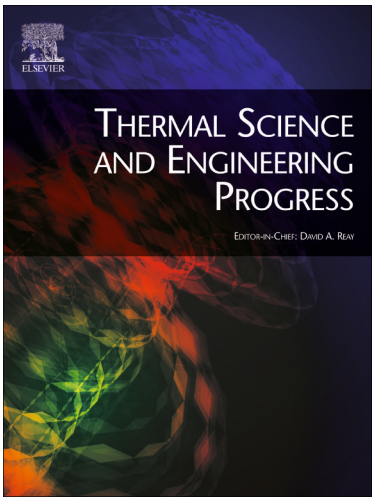

Evaluation of sustainable longan shell biochar energized commercial organic phase change material for low temperature thermal regulation

B Kalidasan, AK Pandey, Imansyah Ibnu Hakim, Nandy Setiadi Djaya Putra, Muhammad Naufal Faris Herviadi, Tan Kim Han, R. Saidur

PII: S2451-9049(26)00200-3
DOI: https://doi.org/10.1016/j.tsep.2026.104674
Reference: TSEP 104674

To appear in: *Thermal Science and Engineering Progress*

Received Date: 10 November 2025
Revised Date: 19 February 2026
Accepted Date: 25 March 2026

Please cite this article as: B. Kalidasan, A. Pandey, I.I. Hakim, N.S. Djaya Putra, M.N. Faris Herviadi, T.K. Han, R. Saidur, Evaluation of sustainable longan shell biochar energized commercial organic phase change material for low temperature thermal regulation, *Thermal Science and Engineering Progress* (2026), doi: https://doi.org/10.1016/j.tsep.2026.104674

Evaluation of Sustainable Longan Shell Biochar Energized Commercial Organic Phase Change Material for Low Temperature Thermal Regulation

B Kalidasan[a,e,*,kalidasanb@sunway.edu.my], AK Pandey[b,**,adarshp@uaeu.ac.ae], Imansyah Ibnu Hakim[d], Nandy Setiadi Djaya Putra[d], Muhammad Naufal Faris Herviadi[d], Tan Kim Han[c], R. Saidur[c]

[a] Sunway Centre for Electrochemical Energy and Sustainable Technology (SCEEST), Faculty of Engineering and Technology, Sunway University, No. 5 Jalan Universiti, Bandar Sunway, 47500, Selangor Darul Ehsan, Malaysia

[b] Mechanical and Aerospace Engineering Department, College of Engineering, United Arab Emirates University, Al Ain 15551, United Arab Emirates

[c] Research Centre for Nano-Materials and Energy Technology (RCNMET), Faculty of Engineering and Technology, Sunway University, No. 5, Jalan Universiti, Bandar Sunway, Petaling Jaya, 47500 Selangor Darul Ehsan, Malaysia

[d] Mechanical Engineering Department, Faculty of Engineering, Universitas Indonesia, Kampus UI DEPOK, 16424, West Jawa, Indonesia

[e] Material Science, Innovation and Modelling (MaSIM) Research Focus Area, North-West University, Mahikeng Campus, Private Bag X2046, Mmabatho 2745, South Africa

[*]Corresponding author at: Sunway Centre for Electrochemical Energy and Sustainable Technology (SCEEST), Faculty of Engineering and Technology, Sunway University, No. 5 Jalan Universiti, Bandar Sunway, 47500, Selangor Darul Ehsan, Malaysia.

[**]Corresponding author.

Graphical abstract

Highlights

2D Longan shell biochar with high specific surface area was synthesized.

Thermal conductance of octadecane improved by 97.89% with 1.2 wt.% of LSB.

PCM-Biochar carbon interaction was discussed with thermophysical analysis.

Abstract

Biochar, lauded for its plentiful raw material availability, compatibility with biological systems, and eco-friendliness, has proven effective in boosting the thermal conductivity of phase change materials (PCMs) and enhancing heat transfer in thermal systems. This paper introduces a distinctive eco-friendly composite PCM with improved thermal conductivity, optical absorbance, and thermal stability, achieved by dispersing laboratory-synthesized longan shell biochar (LSB) using carbonization and melting-mixing methods. LSB microparticles of 0.15-0.16 μm were dispersed at different weight fractions of (0.3; 0.6; 0.9;

1.2 and 1.5 wt.%) blended with commercial octadecane to further enhance the optical and thermophysical behavior. The morphological characteristics, microstructure, optical absorbance and transmittance and thermal properties are characterized. Among the analyzed composites, the octadecane+1.2LSB composite exhibited exceptional chemical compatibility, a significant increase in optical absorbance (from 0.212 to 0.735), and a thermal conductivity enhancement of 97.89% (from 0.142 W/(m·K) to 0.281 W/(m·K)) compared to octadecane; notably, this composite showed a melting enthalpy of 239 J/g without any compensation. The layered sheet-like 3D morphology of LSB along with the mesoporous and micropore surface features a network of sponge-like texture that facilitates the base for stronger intermolecular interaction with the octadecane matrix. Subsequently, the porous structure also contributes to effectively retaining the incident solar rays that enhance the optical absorbance of the composite. The research findings imply that the engineered composite has substantial promise for use in low temperature thermal regulation, presenting an effective and sustainable solution for energy management.

Keywords: Biochar; Composite phase change material; Longan Shell; Thermal energy storage; Thermal performance

Introduction

Thermal energy storage (TES) plays a vital role in enhancing the utilization of renewable energy and improving overall energy efficiency [1]. Utilizing phase change materials (PCMs) for energy storage is a promising alternative, as it can harness insolation as latent heat and resolve persistent issues related to non-conventional energy sources. While there is a variety of organic and inorganic PCMs available, organic PCMs have attracted significant attention from researchers due to their non-toxic properties and thermal stability. PCMs are actively used in solar thermal systems (solar stills [2]; air heaters [3], water heaters), electrical batteries [4] and in buildings for thermal management [5], thermal mitigation and TES. Nonetheless, their low thermal conductivity, low optical absorbance and leakage during the solid-liquid phase limit their application in many areas. Also, cavity formation in PCM during the heat exchange process poses a significant issue as it increases thermal resistance. Furthermore, the presence of these cavities displaces the surrounding PCM, resulting in volumetric expansion and potential leakage.

From a materials standpoint, the integration of thermally conductive nanomaterials stands out as the most common method for enhancing the thermal transfer capabilities of PCMs. Notably, carbon nanomaterials have garnered significant interest due to their low density and remarkable intrinsic thermal conductivity, which ranges from 1000 to 5000 W/(m·K) [6]. Additionally, carbon elements are anticipated to demonstrate enhanced thermal conductivity, influenced by their morphological characteristics such as shape, size, purity, and microstructure. The carbon nanomaterial-based PCM composite shows a significant enhancement effect primarily due to the plentiful sp^2 bonds formed between carbon atoms. The research conducted by Bahiraei et al. [7] indicates that the incorporation of paraffin, a widely utilized organic PCM, with carbon nanomaterials like carbon nanofibers (CNF), graphene nanoplatelets (GNP), and graphite (GP) results in substantial improvements in thermal conductance, showing increases of around 1100% for GP, 284% for GNP, and 168% for CNF. Additionally, a thorough examination reveals that the increase in thermal conductivity for nanometals and nanometal oxides falls within the range of 20% to 160%. Although there have been notable advancements, the prohibitive cost of nano additives hinders their widespread adoption, and the surface modification typically relies on toxic chemicals. The conventional application of nanomaterials faces obstacles such as the synthesis of safer alternatives, the expense associated with raw materials, disposal challenges, and issues related to environmental sustainability and biodegradability. Consequently, when selecting suitable additives, one must

consider both the costs associated with synthesis and the detrimental impact of additives on the latent heat capacity of PCMs. Furthermore, given that the volume of PCM required in a practical TES system far exceeds that in a lab-scale setup, the preferred thermal conductivity enhancers for PCMs should be affordable, easily obtainable, and sustainable. In contrast, biochar offers a renewable, low-cost, and eco-friendly alternative with intrinsic porosity that improves PCM impregnation and reduces leakage.

Transforming waste into valuable products presents a viable approach to reduce environmental harm on both global and local scales while fostering economic growth and societal well-being. Few key applications include waste transfer of natural wood saw dust [8], rice husk/bamboo biochar [9] for polylactic acid hybrid nanocomposite. Biochar is a carbon-dense substance derived from widely available biomass sources such as bamboo, coconut shells [10], and prosopis juliflora [11], along with industrial waste products such as sawdust and paper mill sludge, using a carbonization method in a tube furnace at temperatures between 800-1000 ℃ [12]. Synthesized biochar's are characterized by its adjustable composition and texture, which include high porosity, a surface area that can exceed 1000 m^2g^{-1}, significant cation exchange potential, excellent thermal conductance, and a variety of surface functional groups, positioning it as a key material in the production of carbon based composite PCMs. Biochar-based PCMs are expected to effectively contribute to energy conservation to regulate the environment of greenhouses. However, they are more impactful with higher specific surface area, subsequently longan shell is waste material, that offers a higher specific surface owing to its 2D structure arrangement [13]. Moving forward, a multitude of research efforts focused on biochar synthesis and its use in energy storage sectors have been examined. Guo et al. [14] developed a biochar/CNT blended nanocomposite myristic acid PCM for effective conversion of solar energy storage. In this research, biochar carbon for derived from corn stover and was modified using KOH to use the developed biochar as a porous material carrier. The nanocomposite with myristic acid resulted in enhancing thermal conductance by 40.1% and photothermal energy conversion with 76.37% efficiency. Biochar energized PCM composite was developed by Park et al. [15] to resolve the liquid leakage issue of PCM. Subsequently, this composite was integrated into cross laminated timber, which was intended for thermal regulation application. With biochar blended PCM, the timber board exhibits an increase in energy storage performance of 40% owing to faster thermal response. Likewise, a few remarkable biochar energized composites PCMs and their thermophysical properties are represented using **Table 1** to illustrate a better understanding of performance and their behavior

characteristics. In this regard, this research explores the potential of longan shell derived carbon biochar (LSB) materials in enhancing the thermophysical characteristics of organic PCM for thermal regulation applications. There are few unique features of LSB in comparison to other biochar sources such as coconut, corn waste, rice husk and tea waste etc.

- LSB is different from biochar obtained from other biochar's in terms of its carbon content, surface functional groups, and intrinsic porosity. The elevated lignocellulosic composition of longan shell produces a stable carbon-rich framework with a wealth of oxygen-containing functionalities, which enhances its interfacial compatibility with organic PCMs.
- The 2D mesoporous structure derived from the pyrolysis of longan shells offers an interconnected pore network that is especially advantageous for the impregnation of PCMs. This meso-porosity boosts capillary action, minimizes leakage during phase transitions, and enhances thermal diffusion pathways, effectively tackling two major drawbacks of traditional PCMs: poor thermal conductivity and leakage. (this research work emphasises only on thermal conductivity improvement)

Despite their potential, the commercial nanomaterials discussed earlier encounter critical issues, such as the application of toxic materials during their fabrication, complicated synthesis methods, and high expenses, which undermine environmental sustainability [16]. Drawing from existing literature and research on biochar-based carbon materials, scientists have investigated their potential as both a supporting medium for shape-stabilized (ss) PCMs and as enhancers of thermal conductivity, given their unique microstructure and morphological characteristics. It is important to note that while ss-PCMs can provide improved thermal conductance, a higher proportion of biochar as a supporting material significantly affects the energy storage capacity of the PCM, and at elevated temperatures, the PCMs may lose their shape stability. Conversely, biochar used as a thermal conductivity enhancer can lead to a substantial and optimal increase in thermal conductance without significantly compromising the energy storage capacity of the resulting nanocomposite. This research seeks to explore the viability of incorporating biochar microparticles to improve the thermal conductivity of octadecane as PCM. The biochar was derived from the outer shells of longan fruit, processed at a pyrolysis temperature of 850 °C, and subsequently milled into microparticles. Rich in carbon and featuring a naturally porous structure, longan shells (LS) are abundant and sustainable. The shell of the longan fruit, often overlooked as agricultural waste in Southeast Asia, provides an affordable resource with excellent porosity for PCM retention and robust structural integrity. The composite derived from it functions best at temperatures between 25

°C and 27 °C and can be produced through a straightforward, scalable pyrolysis-impregnation method that is appropriate for commercial use. Given the advantageous properties of biochar and its distinct thermophysical characteristics, it is prudent to explore its potential use in conjunction with PCM and the impact on thermal storage capabilities. To remain competitive with commercial nanomaterials, there is a significant emphasis on developing eco-friendly nanomaterials that exhibit robust thermo-physical characteristics. Consequently, this research focuses on synthesizing an Octadecane/Longan shell biochar nanocomposite PCM that operates at a melting temperature of 28-30 °C, utilizing varying weight fractions of LS microparticle carbon from 0.3 wt.% to 1.5 wt.% through a two-step process. The resulting nanocomposite PCM undergoes characterization to assess its microstructure, morphological properties, chemical stability, optical absorbance, thermophysical attributes (including thermal conductivity, energy storage, and thermal stability), as well as its thermal reliability across 500 phase transition cycles. The developed octadecane/LS sample with 1.2 wt.% biochar carbon exhibits better thermal conductance without compromising the latent heat storage. Subsequently, the optical absorbance of the developed nanocomposite is efficient in comparison to commercial nanomaterials like hexagonal boron and MWCNTs. Furthermore, these nanocomposite exhibits lower density and cost-effectiveness for thermal regulation applications, emphasizing a sustainable future. Economic analysis in support of the developed biochar on comparison with existing commercial nanomaterials is presented in **Appendix I**.

Table 1. Thermophysical characteristics of various biochar enhanced organic PCM as in literature.

Source of Biochar	*PCM*	*PCM Ratio (%)*	*Heat Storage (J/g)*	*Thermal Conductivity W/(m·K)*	*Core Focus*	*Application*	*Reference*
Peanuts Shell Poplar Wood Corn Straw	Stearic Acid	36.82 54.71 65.47	68.6 100.1 114.1	0.530 0.380 0.320	Shape Stabilized PCM	Thermal Energy Storage	[17]
Pinecone	Octadecane	62.21	116.7	-	Shape Stabilized PCM	Building Construction	[18]
Wood Biochar ACQ treated Wood	Polyethylene Glycol-2000	74.93 85.85	96.1 103.3	0.409 0.614	Shape Stabilized PCM	Photo Thermal Energy Conversion	[19]
Coconut shell	A46	99.50	174.6	0.415	Thermophysical Property	Solar Still	[20]
Coconut shell	Polyethylene Glycol-1000	99.00	150.1	0.515	Thermophysical Property	Thermal Energy Storage	[10]
Tea Waste + Cocos Nucifera Oil	Paraffin (OM35)	70.00	150.5	0.129	Form-Stable PCM	Thermal Regulation	[21]
Biochar	Paraffin	90.00	145.3	0.339	Thermophysical Property	Latent Heat Storage System	[22]
Maize Straw	Polyethylene Glycol-8000	85.70	132.0	0.635	Shape Stabilized PCM	Photo and Electro Thermal Energy Conversion	[23]
Phoenix Leaves	Paraffin Stearic Acid Polyethylene Glycol	45.98 53.74 59.37	81.6 92.3 67.6	0.436 0.450 0.409	Shape Stabilized PCM	Thermal Energy Storage	[24]
Date Seed	Eutectic of palmitic acid & Polyethylene Glycol-6000	85.00	202.4	-	Form Stable PCM	Solar Thermal Energy Conversion	[25]
Balsa Wood	Tetradecanoic Acid	60.09	150.3	0.137	Shape Stabilized PCM	Thermal Energy Storage	[26]
Neem Tree	Myristyl alcohol	76.00	186.1	0.673	Form Stable PCM	Battery Thermal Management	[27]
Bamboo Biochar	Soya Wax PCM	60.00	104.3	0.893	Form-Stable PCM	Building Walls	[28]

*ACQ- Alkaline Copper Quaternary

Materials and Methods

Selection of Materials

This research study examines commercial-grade octadecane, a paraffin-based long-chain hydrocarbon PCM with a phase transition temperature of 28-30 ℃, and a latent heat of 230 J/g procured from Suzhou Senfeida Chemical Co. Ltd. It exhibits excellent thermal stability and no supercooling. The octadecane PCM appears in pale whitish color. Biochar produced from the carbonization of longan shells is utilized to enhance thermal conductivity, thereby improving the thermal conductance network within the PCM matrix and increasing optical absorbance.

Synthesis of Longan shell biochar-based carbon microparticle

This section outlines the green synthesis method utilized to transform longan shells into valuable microparticles suitable for efficient energy storage materials. **Figure 1** illustrates the processes involved in the green synthesis of micromaterials from solid waste. Initially, longan shells are sourced from agricultural waste and thoroughly washed with deionized water to eliminate dust and sand, resulting in microparticles with enhanced characteristics. After washing, the longan shells are dried in a vacuum oven at 120 °C for 180 minutes. Subsequently, these shells undergo carbonization to become biochar. The carbonization of longan shells occurs in a nitrogen environment (200 sccm) using high-temperature tube furnace (Nabertherm R50/250/12B14 tube furnace (Germany) at constant heating rate 10°C/min until it reaches a temperature of 900 °C and held for 5 hours in a ensuring an eco-friendly process. The resulting carbonized shells are then further refined through hand crushing and wet ball milling to achieve a smaller particle size. Subsequently, the carbonized longan shells undergo additional refinement through a wet grinding mill. This mill employs zirconia ceramic balls soaked in distilled water to process the sample. A mixture of 10 grams of LS sample, 1 mm zirconia balls, and distilled water are combined in a 1:10:2 volume ratio. The grinding operates continuously at 750 rpm for 15 minutes per cycle, with a 15-minute pause between cycles to allow heat stabilization, for 4 cycles. After milling, the sample is extracted from the bowl and dried in a dry oven at 150 ºC for 180 minutes. The final particle size is analyzed using a particle analyzer, yielding a range of 0.15 – 0.16 µm. The sample is then prepared for subsequent measurements and analysis.

Preparation of Commercial Octadecane/LSB composite PCMs

This section provides a detailed account of the dispersion of the synthesized LS microparticles with commercial octadecane PCM at various weight fractions. Nanocomposite samples weighing 20g are created with LS microparticle weight percentages of 0.3 wt.%, 0.6 wt.%, 0.9 wt.%, 1.2 wt.%, and 1.5 wt.%. The preparation of these samples follows two steps method as depicted in **Figure 2**. Initially, octadecane is precisely measured using a balance and placed in a clean glass beaker. The beaker is then positioned on a hot plate, heated to 80 °C and stabilized for 5 minutes to convert octadecane from solid to liquid, facilitating sonication and mixing. First, LS microparticles are accurately weighed to a specific weight percentage and gradually added to the liquefied octadecane PCM. The mixture is then placed in a sonication device, with the sonication probe immersed in the blend. The device is set to a frequency of 150 kHz with power of 200 W and operates for 60 minutes. This sonication process generates heat, which aids in achieving a uniform dispersion of LS microparticles within the PCM matrix. After the sonication process, the sample is removed and allowed to cool to room temperature. As the composites cool, PCM solidifies, resulting in an even distribution of LS microparticles within the solid PCM matrix. The resulting LS nanocomposites are now ready for further analysis, including morphology, chemical stability, optical absorbance, thermal characterization, and thermal reliability assessments. The complete information regarding the instruments used for characterization is available in **Supplementary Appendix-II**, along with the uncertainty analysis presented in **Supplementary Appendix-III**.

Results and Discussion

This research examines the development of organic PCMs enhanced with LS-based carbon microparticles for effective thermal regulation at low temperatures. Five different octadecane/LS micro composite PCMs, each containing varying amounts of LSB carbon, were created and their thermophysical properties were characterized. The study evaluates aspects such as morphological behavior, chemical stability, thermal conductivity, latent heat, phase transition dynamics, thermal decomposition, and thermal reliability, with findings discussed in the subsequent sections.

Microstructure and Morphology

The morphological behavior and microstructural information of pure octadecane, LSB and its composite with LSB carbon materials are inspected using SEM analysis and BET analysis and are discussed in this section.

Scanning Electron Microscope Analysis

Octadecane, classified as a saturated C18 hydrocarbon PCM, presents a uniform and compact morphology at solid state, exhibits smooth, waxy morphology in solid state with a layered crystalline microstructure as in **Figure 3a** due to its orthorhombic lattice configuration. With the incidence of electron beams the octadecane's temperature slightly increases which causes collapse of octadecane microstructure leading to disorderness and molecular mobility. The LSB's microstructure is observed that it exhibits a layered, sheet-like morphology that resembles a two-dimensional structure. The flakes vary in size and often appear curled or crumpled, indicating significant structural distortion due to carbonization. During the carbonization process of LS, the volatile matter is released leading to shrinkage, cracking of LS which opens the pores in the longan shells. This leads to improved porosity of LSB. The surface features a network of mesopores and micropores, contributing to a sponge-like texture. These pores are randomly arranged and differ in shape some are elongated while others are roughly circular highlighting the heterogeneous characteristics of the biomass precursor. Additionally, cracks and fissures are frequently observed, which improve diffusion pathways and surface reactivity, making this biochar a promising candidate for energy storage. The increase in pores of LSB can be inferred clearly from **Figure 3b**, and this is attributed to the stronger intermolecular attraction as well as the holding of PCM within the pores. A better way to understand is by the keen observation of octadecane and its composite with LSB; the octadecane SEM image tends to illustrate a watery nature where the PCM almost exhibits a nature to melt at 26-27 ℃ and they are clearly observed, whereas in the composite of PCM with LSB, no watery nature is observed, which is clear to understand that the porosity of LSB effectively contributes in holding the PCM within the micropores. Our observations from **Figure 3c** indicate a uniform spread of LSB microparticles across the octadecane matrix, with no signs of agglomeration or clustering. Octadecane penetrates the micropores and mesopores of LS microparticles and intersperses between lamellar structures, promoting enhanced energy storage. The consistent distribution of LSB microparticles generates thermal hotspots within the PCM matrix, which aids in increasing the heat transfer rate. To assess the size and elemental composition of the LS microparticle synthesized through green methods, the microparticle was subjected to testing with a particle sizer and Energy Dispersive X-Ray Analysis (EDX). The results indicate that the size of the LS microparticle ranges from 0.15 to 0.16 μm (as presented in **Supplementary document in Appendix IV)**. EDX findings reveal that microparticles are composed of 88% carbon, with additional elements including O, K, Cl, Ca, Si, Na, and Al, as referenced in **Supplementary S1-S2 and T4 in Appendix V**.

3.1.2 Brunauer–Emmett–Teller Analysis

The specific surface area, pore size, and pore volume distribution of LSB were examined using the BET method in a N_2 adsorption and desorption environment. This section discusses the surface morphological characteristics of LSB, including surface area, pore size, pore volume, DFT pore size, particle size, and pore width. The BET analysis indicates that the synthesized LSB contains voids that range in size from nanoscale to microscale. These voids are typically classified into micro, meso, and macropores based on their respective size ranges of 2 nm to 50 nm. Additionally, it is noted from **Figure 4a** that at lower relative pressure levels, the activated LSB shows reduced adsorption of nitrogen gas. As the relative pressure increases, the adsorption of nitrogen gas also rises. The activated biochar exhibits hysteresis loops in their adsorption and desorption curves, which align with type IV curves as per IUPAC standards. The highest values for adsorption and desorption are observed at a relative pressure (p/p^o) between 0.96 and 1.0. Furthermore, the DFT pore size distribution corroborates a significant mesoporous distribution for LSB, with most pores falling within the 2–3 nm range as in **Figure 4b**.

Based on the results from BET analysis, LSB has a surface area of 121.1530 m^2/g, a pore volume of 0.029258 cm^3/g, and an average pore diameter of 2.5419 nm. The pore size of LSB is like that of other biochar's utilized in the synthesis of form-stable composite PCM. Its specific surface area and pore volume make the activated biochar a promising candidate for absorbing and containing PCM as a supporting material. However, the primary focus of this research is to improve the thermo-physical properties of commercial grade octadecane PCM. The higher BET surface area allows for increased liquid PCM adsorption within the pores. The capillary force and surface tension of the porous media aid in the absorption of liquid PCM particles. BET analysis shows that the mesoporous structure of activated LSB effectively absorbs liquid PCM.

Chemical Stability Evaluation

To investigate the functional groups within octadecane, LSB, and PCM+LSB samples, Fourier transform infrared spectroscopy (FT-IR) was utilized. A chemical fingerprint is

generated through FTIR by assessing the amount of light absorbed by the bonds of vibrating molecules, specifically by examining the infrared portion of the electromagnetic spectrum and is presented in **Figure 5**. Overall, in the octadecane sample only four spectral peaks occur, among which two are steep and two are smaller ones. The presence of IR rays results in notable peaks at wavenumbers 2917 cm^{-1}, 2849 cm^{-1}, 1466 cm^{-1}, and 719 cm^{-1}. These peaks align with those found in paraffin samples, which are classified under the alkane group. The significant peaks at 2917 cm^{-1} and 2849 cm^{-1} are attributed to the $-CH_3$ and $-CH_2$ functional groups, demonstrating their symmetric stretching vibrations in the presence of IR rays. The smaller peak at 1466 cm^{-1} signifies the bending deformation modes of the $-CH_2$ and $-CH_3$ groups, while the peak at 719 cm^{-1} indicates the rocking vibrations of the $-CH_2$ group when exposed to IR radiation in FTIR analysis. Followed by the PCM sample is the chemical peak analysis of LSB carbon source, where the spectral curves don't represent any spectral peaks, this clearly indicates that the nano powder opted for the research is not IR active and does not reflect any peaks in the electromagnetic spectrum. As both biochar and activated carbon are types of amorphous carbon with high porosity, they are structurally indistinguishable from one another. In contrast to activated carbon, biochar typically contains a rich array of surface functional groups such as C-O, C=O, COOH, and OH. These groups are highly adaptable, serving as a foundation for the creation of diverse functionalized carbon materials. Currently, the Logan shell biochar nanomaterial produced does not incorporate modifications through functionalization elements and is synthesized without further chemical processing. This leads to the surface functional groups, such as C-O, C=O, and COOH, becoming inactive, as the biochar is synthesized at a high temperature of 800 °C in a tube furnace. As a result, these functional groups exhibit low activity, which is reflected in FTIR analyses conducted in the fingerprint and functional group regions. Subsequently, all the nanocomposite of PCM and LSB carbon powder denotes peaks in correspondence to the ones observed in octadecane PCM, and there are no new peaks or modifications observed in the spectral plots of PCM nanocomposite. This leads us to conclude that PCM and LSB carbon powder do not undergo any chemical reaction, indicating their favorable chemical compatibility. Improving the thermal conductivity of organic PCMs is essential. Moreover, it is confirmed that during ultrasonication, the bonding between PCM and nano powder occurs only through physical interactions that exploit capillary and surface tension forces between the materials. The absence of new peaks in FTIR confirms a predominant physical interaction between LSB and octadecane; however, future studies exploring chemically activated or functionalized

biochar could introduce additional surface functional groups, thereby strengthen interfacial bonding and further enhance thermal performance

Optical Absorbance and Transmittance

Optical absorbance and transmittance analysis of PCM and the nanomaterial dispersed nanocomposite PCM are insightful in understanding the ability of the PCM to behave under the electromagnetic spectrum. Application of the developed PCM composites towards solar thermal energy-based application systems are determined based on this analysis. The spectrum of solar radiation is primarily made up of ultraviolet (UV) rays, visible rays, and near-infrared (IR) rays, which represent 7%, 44%, and 37% of the total, respectively. Therefore, the optical characteristics of the developed composites are assessed within the wavelength range of 280–1400 nm. The patterns of photo absorptivity and transmittance for the PCM nanocomposites are analyzed using a UV-Visible spectrometer and are presented in **Figure 6a** and **Figure 6b**.

The optical absorbance plot in **Figure 6a** presents the spectral curves obtained for octadecane and its composite with LSB, the average of the absorbance between wavelength 280-1400 nm ensures the optical absorbance of octadecane to be 0.212 (which is very low on consideration to apply for solar thermal application for effective harnessing). Subsequently, with LSB of 0.3 wt.%, 0.6 wt.%, 0.9 wt.%, 1.2 wt.% and 1.5 wt.% the optical absorbance of octadecane surges to 0.504, 0.528, 0.676, 0.735 and 0.748 respectively. The increment contributes to an increase in absorbance of about 137.74%, 149.06%, 218.87%, 246.70% and 252.83% respectively, which is owing to the following scientific implications. a) the LSB biochar carbon material is characterized by π-conjugated carbon structures, which effectively boost optical absorption in the UV-Vis-NIR spectrum [29]; b) surface morphology of LSB is characterized by its porous and irregular nature, which facilitates light scattering and trapping, ultimately boosting the optical absorbance of the octadecane-biochar composite [30]; and also c) the even distribution of biochar in octadecane results in a heterogeneous mixture that interferes with light transmission and enhances absorbance through interfacial polarization effects [31]. On a keen note, the increase in optical absorbance subsequently influences the optical transmittance of octadecane and this is evident from the optical transmittance plot presented in **Figure 6b**. GNB effectively increases the absorbance with significant positive notes by decreasing the transmittance of the developed composite. Based on the optical transmissibility plot as presented in Figure 4b, herein a comparison between the transmissibility

obtained from UV-Vis analysis and the solar spectrum value is conducted to determine an optical transmissibility of 60.75 % for octadecane PCM. The introduction of LSB carbon material at various weight percentages of 0.3 wt.%, 0.6 wt.%, 0.9 wt.%, 1.2 wt.%, and 1.5 wt.% caused a marked decline in optical transmissibility, resulting in measurements of 30.3%, 28.8%, 20.3%, 18.0%, and 17.2%, respectively. When radiation interacts with a medium, it can be transmitted, absorbed, or reflected. Octadecane being organic material typically is transparent, allowing radiation to pass through them. There is a negative correlation between absorbance and transmissibility; therefore, modifying PCMs with LSB decreases their transmission capabilities, which in turn increases their absorbance. This enhanced absorptivity improves the material's responsiveness to solar radiation, leading to a faster rate of TES.

Thermal Properties

For PCMs, thermal properties are of utmost importance as PCMs facilitate thermal energy storage involving the influence of thermal conductance (charging/discharging rate), melting temperature (operational temperature), latent heat (energy storage potential), thermal stability (degradation initiation point) and thermal reliability (ability to operate on long term). This section of the article discusses the above-mentioned thermal characteristics of Octadecane and its nanocomposite with LS micro particle.

Thermal Conductivity

Thermal conductivity is characterized as the fundamental property of a material that enables heat transfer across a temperature gradient, and it is impacted by several elements such as the material's microscopic structure, phase, density, and the temperature at which it operates. A transient hot bridge instrument is used to measure the thermal conductance of low temperature octadecane sample via transient hotwire technique. The thermal conductivity of commercial octadecane and its nanocomposites with LS carbon material is depicted in **Figure 7**. According to the graph, the thermal conductivity of octadecane PCM is measured at 0.142 W/(m·K), indicating the need for a filler material to boost thermal performance. The use of green synthesized microparticles of LSB carbon at varying concentrations of 0.3 wt.%, 0.6 wt.%, 0.9 wt.%, 1.2 wt.%, and 1.5 wt.% has greatly improved the thermal conductivity of commercial octadecane PCM, resulting in thermal conductivities of 0.173 W/(m·K), 0.198 W/(m·K), 0.224 W/(m·K), 0.281 W/(m·K), and 0.263 W/(m·K) correspondingly. On a keen observation it can be inferred that octadecane with 1.2 wt.% of LSB carbon material depicts an increase in thermal conductance by 97.89%. The thermal conductivity of the octadecane/LS PCM composite improves as the weight fraction of LSB microparticles increases up to 1.2

wt%. This enhancement is attributed to two main factors: a) the uniform distribution of the highly conductive LS filler materials creates thermal networks within the octadecane matrix, facilitating heat transfer [32]; b) the porous structure of LSB results in a higher surface area relative to its volume, which enhances the mobility of the LS microparticles and promotes phonon interactions for effective heat conduction [33].

On the other hand, it is observed that when the concentration of LS microparticles at 1.2 wt.% in octadecane is increased, there is a notable decline in the thermal conductivity of the composite produced, which is significant enough to warrant discussion. At this higher concentration, two key phenomena take place: a) the cohesive forces among the LS microparticles intensify, resulting in cluster formation that gradually expands into denser molecules, and due to agglomeration, these clusters settle during repeated phase transitions, thereby disrupting the uniform distribution required for optimal thermal conduction [34]; and b) the mean free path for intermolecular diffusion becomes constrained due to the increased density of the composite PCM. The thermal conductivity obtained reflects an improvement in heat transfer performance, yet a limited presence of nanoparticles might be insufficient for achieving exceptional heat transfer results. In upcoming research, infrared thermography will be utilized to illustrate the surface temperature distribution of consolidated PCM composites, allowing for a more thorough evaluation of thermal uniformity in real-world operating conditions.

Phase Transition Enthalpy

The thermal properties associated with phase changes, such as melting enthalpy (ΔH_m) and cooling enthalpy (ΔH_c), along with the phase transition temperature (T_m) of the developed LS microparticle dispersed composite PCMs, were analyzed using a DSC instrument. **Figure 8** illustrates the heat flow curves for octadecane and octadecane/LS composites at various weight fractions during the phase transition process. A crucial aspect in determining the effectiveness of PCM for energy storage lies in the enthalpy of phase change. Materials that possess a higher enthalpy for phase transitions can accumulate more energy, and the efficiency of this enthalpy during the energy release phase after charging is critically important. **Figure 8** shows an endothermic peak that reflects the PCM's absorption of thermal energy from its surroundings, leading to a phase change from solid to liquid and the storage of that energy. The following

exothermic peak indicates the release of this stored thermal energy as the PCM transitions back to a solid state. A single peak of phase transition is noted, signifying that the PCM experiences solely a solid to liquid transition. The DSC curves of the composite PCMs resemble those of the original PCMs, albeit with variations in their position and height, suggesting that the addition of biochar has influenced the melting and solidification temperatures as well as the heat enthalpies. Following the incorporation of LSB, the melting and solidification temperatures of the PCMs were modified to varying extents, as detailed in **Table 2**, which is derived from **Figure 8**.

The phase transition temperature of commercial octadecane is around 31-33 ℃, with onset melting temperature being about 23-26 ℃, which is in accordance with the values defined by the material provide. Subsequently, inferring the composite samples ensures that there is a slight edge in onset of phase transition to begin with dispersion of LSB owing to improved thermal conductance. However, the variation in temperature for both onset temperature as well as for peak melting temperature are within 0.5-1.0 ℃, which is very common owing to the entropy generation. Analysis of the melting phase shows that both octadecane and the LS dispersed composite PCM present a single endothermic peak, implying that isomorphous structures are present in both the octadecane and the composites.

Table 2. Thermophysical properties of Octadecane and Octadecane/LS composites characterized using DSC.

Samples	$T_{onset\ melt}$ ℃	$T_{peak\ melt}$ ℃	$T_{onset\ freeze}$ ℃	$T_{peak\ freeze}$ ℃	ΔH_{melt} (J/g)	ΔH_{freeze} (J/g)	*Energy storage efficiency (%)*
Octadecane	23.4	34.7	25.6	17.1	240.9	-236.3	98.09
Octadecane+0.3 LSB	23.6	33.8	25.8	18.7	247.3	-241.0	97.45
Octadecane+0.6 LSB	24.1	33.5	24.5	16.8	244.5	-240.9	98.52
Octadecane+0.9 LSB	23.5	34.1	25.8	17.2	240.4	-235.4	97.92
Octadecane+1.2 LSB	24.0	33.6	24.8	15.8	239.0	-233.2	97.57
Octadecane+1.5 LSB	23.5	34.0	24.7	15.9	228.7	-221.6	96.89

Alongside the phase transition temperature, the melting/freezing enthalpy is a crucial thermal property. As indicated by the vendor, octadecane has a melting enthalpy (ΔH_{melt}) of 240 J/g and a freezing enthalpy (ΔH_{freeze}) of 236 J/g. The reports show that the melting enthalpy (ΔH_{melt}) values for the LS carbon material dispersed composite PCM at concentrations of 0.3 wt.%, 0.6 wt.%, 0.9 wt.%, 1.2 wt.%, and 1.5 wt.% are 247.3 J/g, 244.5 J/g, 240.4 J/g, 239.0 J/g, and 228.7 J/g, respectively. Similarly, the freezing enthalpy (ΔH_{freeze}) values for the same concentrations are -241.0.2 J/g, -240.9 J/g, -235.4 J/g, -233.2 J/g, and -221.6 J/g, respectively.

Curiously, the composite exhibits an increase in melting and freezing enthalpy with less quantity of LSB content, however the enthalpy considerably drops with higher fraction of LSB content which calls for scientific interpretation. The rise in melting enthalpy of octadecane at a 0.3 wt.% dispersion of LSB is mainly attributed by a) biochar's 2D platelet structure and elevated carbon content, which aids heterogeneous nucleation, improve crystallinity, and encourage molecular organization during the solid-liquid phase change; b) furthermore the strong interactions at the interface and lower chain mobility close to the biochar surface result in superior latent heat storage [35]. Additionally, the well-distributed structure prevents phase separation and aggregation, promoting effective thermal energy capture and release. However, with an increase in LSB content above 0.3 wt.% the melting enthalpy depicts a decreasing trend, which is attributed by the dominance in replacement of energy storage materials (PCM) by the thermal conductivity enhancer material. If the intermolecular interaction strength between octadecane and LSB molecule is greater than the mass of the octadecane that has been substituted by LSB, the latent heat of the composite will increase. In contrast, if the mass replaced is greater than the strength of the intermolecular interaction between octadecane and LSB, the latent heat will decrease. At lower concentrations, the intermolecular interactions dominate over the mass displaced, resulting in an increase in latent heat capacity. However, as concentration rises, the latent heat decreases because of the increased mass of PCM being replaced. As well, the freezing temperature of octadecane and the developed composites are at the range of 24-26 ℃ which is also the onset phase transition melting temperature. This ensures that octadecane and the composites are free from challenge of degree of supercooling, which enhances its ability to be used for real-time application. Finally, the energy storage efficiency which defines the ability of the PCM to support maximum utilization of the thermal energy stored during PCMs phase transition from solid to liquid state. This is calculated using the simple formula (ΔH_{freeze}/ ΔH_{melt})*100. As a result, the energy storage efficiency of all the composite is more alike to that of commercial PCM, as well they are about 96-98% which is far superior to the energy storage efficiency of certain salt hydrate PCMs which are in the range of 75-85%.

Thermal Stability

Ensuring the thermal stability of PCM is vital for the effective operation of the system on a practical level. This research examines the thermal stability of pure PCM in comparison to biochar composite PCM. The experiments for all samples are performed within a temperature range of 30 °C to 350 °C, at a ramp rate of 10 °C/min under N_2 atmospheres using the TGA

instrument. The weight decomposition results are depicted against temperature in **Figur**e **9**. Analysis of the TGA curve indicates that octadecane and its micro composite undergo a single-step degradation. It was logical that the immaculate n-octadecane experienced just a simple evaporation technique. The composite samples maintain significant thermal stability with negligible weight loss until reaching 150°C, after which octadecane and LS composites start to degrade with minimal temperature change. As can be inferred from **Figure 9**, the pure PCM is fully degraded at 234℃, while the composite retains a minor residue that reflects the undecomposed additives, namely LSB, in the composite with different weight ratios. This observation confirms that the composite's components have been thoroughly integrated. Furthermore, the addition of biochar causes the TGA curve to shift to a higher onset degradation temperature, demonstrating enhanced thermal stability of the biochar composite PCM.

During the decomposition process, octadecane decomposes by almost 97-98% between the temperature range of 170-235 ℃ as it breaks from long chain hydrocarbon to monomers. Likewise, with LSB, the developed composites exhibit an increased decomposition initiation point. On a keen note, all the composite samples retain their mass until 170 ℃, which is almost 20 ℃ above the breakdown initiation temperature of pure octadecane. Subsequently, the final or the maximum degradation temperature for the samples with LS at weight fraction of 0.3 wt.%, 0.6 wt.%, 0.9 wt.%, 1.2 wt.% and 1.5 wt.% are depicted to be 240 ℃, 243 ℃, 243 ℃, 234 ℃, and 245 ℃. There is an irregularity in the final degradation temperature of the composite sample with respect to the weight fraction of LSB carbon material, which could be owing to the sampling taken for TGA analysis, as the samples are almost less than 5 mg, these changes are expected to occur. Nevertheless, the inference in increase in initial and final temperature of degradation with LSB can be attributed due to a) ability of LSB carbon to act as thermal barrier and delay breakdown of polymers; b) porous structure of LSB carbon material promotes char formation and reduces the volatile degradation pathway. Concerning real-time operational conditions, octadecane along with the developed composite is designed to operate effectively within a temperature range of 27-40 °C, which is nearly 4-5 times below the initial degradation temperature. This confirms the stability and potential of the developed composite samples for use in real-time thermal regulation.

Thermal Reliability

This research confirms that biochar, due to their porous nature and cost-effectiveness, enhance the thermal performance of composites, nevertheless it is important to analyze their performance with repeated operation. This section of the research emphasis on the performance of PCM in terms of thermal reliability. Furthermore, the effectiveness of the developed composite relies on its stability and capacity to maintain its thermophysical properties over extended use without any degradation, making thermal reliability assessment crucial. Octadecane and its composite with LSB carbon material at optimized weight fraction is considered and herein an accelerated thermal cycling is conducted with continuous heating and cooling within the temperature range of 05℃ to 60℃. As octadecane is intended for low temperature thermal regulation operation, the accelerated thermal cycling is performed manual by sudden heating and cooling. After 200 thermal cycles, octadecane and the composites with LS are evaluated to understand the chemical stability, optical absorbance ability, energy storage potential and thermal stability based on its degradation temperature as presented in **Figure 10**.

It can be inferred from **Figure 10a** that octadecane and LS composite with octadecane reflect 4 peaks under FTIR spectrum which are alike to the peaks obtained prior to thermal cycling for similar samples. We notice two intense sharp peaks at wavenumber 2917 cm^{-1} and 2850 cm^{-1}, as well as two small sharp peaks at wavenumber 1470 cm^{-1} and 717 cm^{-1}. The replica being a similar pattern ensures that the PCM composite are chemical stability even with long term operation. Next from **Figure 10b**, the optical absorbance is evaluated after thermal cycling, it is noticed that there is a significant drop in optical absorbance of octadecane from 0.212 to 0.152 (which contributes to about 28.3%); whereas for octadecane+1.2LS composite the optical absorbance depicts a slight dive from 0.735 to 0.653 (about 11.1%). Furthermore, on evaluating the transmissibility it is inferred that octadecane exhibits 71.8% transmittance from 60.75% after thermal cycling, whereas octadecane+1.2LSB exhibits only 21.7% from 18.0%. The above optical characteristics clearly depict that the composite PCM exhibits better performance when compared to pure octadecane owing to the presence of biochar carbon content, that still retains its ability to absorb visible light. Furthermore, **Figure 10c** displays the heat flow curve of PCM and the composite after thermal cycling. On keen observations we notice drop in energy storage potential by 3-4% which is under permissible limit, however we don't notice significant changes in the phase transition temperature, which is a positive note to consider while choosing PCM for real-time application. Regarding the assessment of thermal stability, the PCM composite demonstrates consistent stability up to 150 ℃, maintaining a comparable initial degradation temperature

prior to thermal cycling. However, after undergoing 200 thermal cycles, there is a minor reduction in the final degradation temperature by 1-2 ℃ as can infer from **Figure 10d**. Furthermore, even after prolonged use, both the PCM and its composites display a single-step degradation process, which is preferable for ensuring their thermal stability performance. The results obtained from PCM and its composite with LSB after thermal cycling are encouraging, indicating the reliability of the developed samples for practical use and long-term operations. The sample demonstrates its thermal reliability for extended use, making the developed composite suitable for low-temperature thermal regulation and heat management in buildings through the integration of PCM layers in roofs, walls, and extruded elements.

Conclusion

In this research investigation, a novel sheet-like carbon structure resembling two-dimensional flakes was successfully synthesized from longan shell biomass using a green and sustainable approach. The resulting microparticles exhibited hierarchical mesoporous and microporous architectures with abundant surface functional groups, enabling strong interactions with octadecane through a two-step incorporation process. These structural features played a decisive role in enhancing the thermo-physical behavior of the composite PCM. Notably, the biochar–octadecane composite demonstrated a 246.7% increase in optical absorbance and a 97.89% improvement in thermal conductivity, while largely maintaining its latent heat storage capacity. The thermal stability of the composite was further validated through 200 melt–freeze cycles, confirming its suitability for long-term use in energy storage and thermal regulation systems. When viewed in the broader context of PCM research, these improvements highlight the potential of agricultural-waste-derived biochar as a low-cost, renewable, and environmentally responsible additive for enhancing PCM performance. Unlike conventional polymeric encapsulation strategies that often compromise latent heat capacity at higher loadings, the porous architecture of LSB facilitated improved thermal transfer pathways without severely diminishing energy storage capability. This positions the developed composite as a promising candidate for solar energy harvesting, passive building cooling, and other real-world thermal management applications where cost-effectiveness and sustainability are equally important.

Nevertheless, the present work also reveals certain limitations. At higher filler loadings, a marginal reduction in latent heat was observed, and prolonged cycling led to slight degradation of optical absorbance, which may limit performance in demanding long-term applications. Future studies could address these issues by optimizing the biochar loading fraction, employing

surface functionalization to improve interfacial compatibility, or designing hybrid filler systems to simultaneously enhance leakage resistance and cycling durability. Additionally, systematic exploration of uniformly sized LS derived 2D flakes with controlled mesoporosity could further advance the energy storage potential while ensuring structural stability. Overall, this work not only demonstrates the value of longan shell waste as a sustainable carbon source but also underscores the broader scientific and practical implications of biochar-engineered PCMs in the pursuit of efficient, eco-friendly, and scalable thermal energy storage solutions.

Acknowledgement

Sunway University authors acknowledge the financial assistance of Sunway University and Universitas Indonesia through SU-UI Bilaterial Strategic Alliance Matching Grant Scheme (GRTIN-UI-RCNMET-09-2024) for carrying out this research. This work is also supported by National Key Research and Development Program of China (2024YFE0208500).

Reference

1. Pandey, A., et al., *Graphene nanoplatelets-infused binary eutectic phase change materials for enhanced thermal energy storage.* Materials Today Sustainability, 2024. **27**: p. 100934.
2. Murali, G., et al., *Improved solar still productivity using PCM and nano-PCM composites integerated energy storage.* Scientific Reports, 2024. **14**(1): p. 15609.
3. Murali, G., et al., *Experimental studies on solar reusable can air heating system integrated with latent heat storage.* Journal of Thermal Analysis and Calorimetry, 2024. **149**(16): p. 8865-8872.
4. Masthan Vali, P., et al., *Synthesis and Characterization of Paraffin Wax-Based Composite Phase Change Materials With Improved Thermal Properties for E-Vehicle BTMS.* Energy Science & Engineering, 2025. **13**(11): p. 5731-5740.
5. Vali, P.M. and G. Murali, *Experimental study on thermal management of nano-enhanced phase change material integrated battery pack.* ASME Journal of Heat and Mass Transfer, 2024. **146**(3): p. 032401.
6. Han, G.G., H. Li, and J.C. Grossman, *Optically-controlled long-term storage and release of thermal energy in phase-change materials.* Nature communications, 2017. **8**(1): p. 1446.
7. Bahiraei, F., A. Fartaj, and G.-A. Nazri, *Experimental and numerical investigation on the performance of carbon-based nanoenhanced phase change materials for thermal management applications.* Energy Conversion and Management, 2017. **153**: p. 115-128.
8. Vengadesan, E., et al., *Hybrid bio-composites reinforced with natural wood saw dust and eco-friendly graphite: evaluation of physical, mechanical, and thermal properties.* Fibers and Polymers, 2025. **26**(2): p. 833-854.
9. Vengadesan, E., et al., *Rice husk and bamboo biochar-reinforced polylactic acid hybrid composites: Evaluation of mechanical, thermal, and physical properties.* Express Polymer Letters, 2025. **19**(8).

10. Kalidasan, B., et al., *Green synthesized 3D coconut shell biochar/polyethylene glycol composite as thermal energy storage material.* Sustainable Energy Technologies and Assessments, 2023. **60**: p. 103505.
11. Yadav, A., et al., *Optimizing Thermal Properties and Heat Transfer in 3D Biochar-Embedded Organic Phase Change Materials for Thermal Energy Storage.* Materials Today Communications, 2024: p. 108114.
12. Atinafu, D.G., et al., *Engineering biochar with multiwalled carbon nanotube for efficient phase change material encapsulation and thermal energy storage.* Energy, 2021. **216**: p. 119294.
13. Lv, L., et al., *Effect of structural characteristics and surface functional groups of biochar on thermal properties of different organic phase change materials: Dominant encapsulation mechanisms.* Renewable Energy, 2022. **195**: p. 1238-1252.
14. Guo, W., et al., *Eco-friendly biochar/CNTs-enhanced myristic acid composite phase change materials for efficient solar-thermal energy conversion.* Solar Energy, 2025. **294**: p. 113483.
15. Park, J., S.J. Chang, and S. Kim, *Enhancing thermal performance of cross-laminated timber using phase change materials and biochar composites.* Journal of Energy Storage, 2025. **109**: p. 115198.
16. Poyyamozhi, N., et al., *Comparative analysis of salt gradient solar pond energy storage and PCM-coupled TiO2 nanoparticles for enhanced solar energy utilization.* Journal of Thermal Analysis and Calorimetry, 2025: p. 1-9.
17. Sun, M., et al., *Evaluation into the effect of lignocellulosic biochar on the thermal properties of shape stable composite phase change materials.* Industrial Crops and Products, 2024. **222**: p. 119961.
18. Katish, M., et al., *Experimental study of phase change material (PCM) biochar composite for net-zero built environment applications.* Cleaner Materials, 2024. **14**: p. 100274.
19. Zhang, Z., et al., *Novel phase change materials with superior thermal conductivity and photothermal efficiency derived from preservative-treated wood biochar.* Renewable Energy, 2024. **237**: p. 121724.
20. Rajamony, R.K., et al., *Energizing solar still efficiency with eco-friendly coconut shell biochar enhanced organic phase change material.* Separation and Purification Technology, 2025. **360**: p. 131200.
21. Arman, Z., et al., *Green form-stable biocomposite of biochar from tea industry waste and organic phase change material.* Journal of Energy Storage, 2024. **101**: p. 113815.
22. Lv, L., S. Huang, and H. Zhou, *Performance investigation of biochar/paraffin composite phase change materials in latent heat storage systems: Feasibility of biochar as a thermal conductivity enhancer.* Journal of Energy Storage, 2024. **91**: p. 112106.
23. Zhang, J., et al., *Light-and electro-driven phase change materials derived from activated porous biochar nanosheets and encapsulated polyethylene glycol.* Colloids and Surfaces A: Physicochemical and Engineering Aspects, 2024. **690**: p. 133783.
24. Lv, L., S. Huang, and H. Zhou, *Effect of introducing chemically activated biochar as support material on thermal properties of different organic phase change materials.* Solar Energy Materials and Solar Cells, 2024. **264**: p. 112617.
25. Gowthami, D., et al., *Development of a novel form-stable phase change material based on alkali activated date seed biochar to harvest solar thermal energy.* Journal of Energy Storage, 2024. **83**: p. 110699.
26. Xu, Q., et al., *Muscle supercompensation inspired high-strength partially dissolved-regenerated cellulose biochar as the matrix of phase change materials for thermal storage.* Sustainable Materials and Technologies, 2023. **38**: p. e00710.
27. Goud, M. and F. Raval, *A sustainable biochar-based shape stable composite phase change material for thermal management of a lithium-ion battery system and hybrid neural network modeling for heat flow prediction.* Journal of Energy Storage, 2022. **56**: p. 106163.
28. Vengadesan, E., K. Gnanasekaran, and S. Muralidharan, *Activated bamboo biochar-infused soy wax PCM: A green composite with enhanced thermal conductivity for thermal energy storage applications.* Materials Letters, 2025: p. 138991.
29. Balasubramanian, K., et al., *Tetrapods based engineering of organic phase change material for thermal energy storage.* Chemical Engineering Journal, 2023. **462**: p. 141984.

30. Kumar, R., et al., *A comparative study on thermophysical properties of functionalized and non-functionalized Multi-Walled Carbon Nano Tubes (MWCNTs) enhanced salt hydrate phase change material.* Solar Energy Materials and Solar Cells, 2022. **240**: p. 111697.
31. Gao, H., et al., *Energy harvesting and storage blocks based on 3D oriented expanded graphite and stearic acid with high thermal conductivity for solar thermal application.* Energy, 2022. **254**: p. 124198.
32. Tong, X., et al., *Organic phase change materials confined in carbon-based materials for thermal properties enhancement: Recent advancement and challenges.* Renewable and Sustainable Energy Reviews, 2019. **108**: p. 398-422.
33. Islam, A., et al., *Investigating the thermal properties of bio-waste derived leak-proof composite phase change material for thermal energy storage: A. Islam et al.* Journal of Thermal Analysis and Calorimetry, 2025: p. 1-18.
34. Shen, Z., et al., *Enhanced thermal energy storage performance of salt hydrate phase change material: effect of cellulose nanofibril and graphene nanoplatelet.* Solar Energy Materials and Solar Cells, 2021. **225**: p. 111028.
35. Liang, Q., D. Pan, and X. Zhang, *Construction and application of biochar-based composite phase change materials.* Chemical Engineering Journal, 2023. **453**: p. 139441.

Figure 1. Synthesis process of LSB

Figure 2. Preparation of Octadecane+LS composite PCMs

Figure 3. Morphological and microstructural appearance of a) Octadecane (PCM) (100 µm); b) Longan shell biochar (thermal conductivity enhancer) (100 µm); and c) composite of Octadecane/LSB (05 µm).

Figure 4. BET analysis a) adsorption-desorption isotherms of LSB; b) pore size distribution.

Figure 5. *Chemical stability evaluation of PCM, LSB carbon powder and their nanocomposite.*

Figure 6. *Optical features of developed nanocomposite PCM a) absorbance and b) transmittance.*

Figure 7. Thermal conductivity of Octadecane and its LSB dispersed nanocomposite along with incremental percentage.

Figure 8. Heat flow curve of Octadecane and its composite with LSB carbon retrieved from DSC instrument.

Figure 9. Thermal stability analysis of PCM and its composite with reference to the degradation temperature.

Figure 10. Thermal reliability analysis of Octadecane and its optimized composite with 1.2 wt.% of LSB using a) Chemical stability evaluation; b) Optical absorbance; c) Heat flow curve and d) Thermogravimetric analysis.